

# Modeling transport of interstitial potassium in regional myocardial ischemia: effect on the injury current

Mark Potse,<sup>1,2</sup> Ruben Coronel,<sup>3</sup> A.-Robert LeBlanc,<sup>1,2</sup> and Alain Vinet<sup>1,2</sup>

**Abstract**—Myocardial ischemia leads to an efflux of potassium ions from affected cells. The resulting depolarization of the resting membrane is one of the main features of ischemic myocardium. It has been shown experimentally that a part of the surplus interstitial potassium is transported out of the ischemic zone, even if no coronary blood flow is present in the affected area. We propose to model this transport mechanism mathematically with a diffusion equation. This model explains the measured spatial profiles of extracellular potential and potassium concentration. In addition, it allows a quantitative prediction of the transmembrane current that flows as a result of ischemia-induced depolarization. This current is thought to play a role in arrhythmogenicity, which is an important cause of mortality in acute myocardial infarction. Our model predicts that this current reaches its maximum exactly on the border of the hypoxic area. An important depolarizing current would be present just within the border, where hypoxia is accompanied by a resting membrane potential that is only slightly elevated, due to coupling with the adjacent normal tissue. Still, in the presence of potassium transport the predicted current density is not large enough to explain ectopic activation on the lateral border of the ischemia. This suggests that activation is more likely to occur at the endocardium, where the potassium gradient is steeper.

## I. INTRODUCTION

Among the numerous electrophysiological changes that take place in ischemic myocardium [1], the increase in extracellular  $K^+$  concentration ( $[K^+]_o$ ) [2] is one of the most important. Increased  $[K^+]_o$  leads to a less negative resting membrane potential ( $V_m$ ). The resulting “injury current,” which flows between the ischemic and non-ischemic tissue, is thought to play a role in arrhythmogenesis during acute myocardial ischemia [3]. A quantitative understanding of this phenomenon requires an accurate mathematical model of the ischemic zone, because the transmembrane current ( $I_m$ ) is very sensitive to some simplifying assumptions that are commonly made. The simplest assumption, a uniform offset of  $V_m$ , would lead to infinite  $I_m$  on the border and zero  $I_m$  everywhere else. Ad-hoc profiles have been used to obtain a smoother transition [4], [5]. These lead to finite current, but the amplitude of  $I_m$  is still as arbitrary as the chosen profile. We have recently introduced a quantitative model of  $[K^+]_o$  [6]. This model leads to realistic profiles of  $[K^+]_o$  and  $V_m$ . In this study, we use our model to predict the spatial profile of  $I_m$  in the ischemic border zone.

From the <sup>1</sup>Research Center, Hôpital du Sacré-Cœur de Montréal, 5400 Boulevard Gouin Ouest, Montréal (Québec) H4J 1C5, Canada; <sup>2</sup>Institute of Biomedical Engineering, Université de Montréal, PO Box 6128, station Centre-ville, Montréal (Québec) H3C 3J7, Canada; and <sup>3</sup>Laboratory of Experimental Cardiology, Center for Heart Failure Research, Academic Medical Center, Amsterdam, The Netherlands.

## II. METHODS

Simulations were performed with a bidomain membrane-based reaction-diffusion model described previously [7]. We used the 2004 version of the TNNP model of the human ventricular myocyte to compute ionic currents [8]. Simulations were performed in a slab of tissue that was 4 cm wide and long, and 1 cm thick, on top of a tissue bath that was 2 cm deep (Fig. 1). This rectangular setup was to mimic the ventricular wall, while avoiding the difficulties of representing results in an anatomically realistic model. For an optimal match with the real heart, a “transmural” fiber rotation of  $120^\circ$  was applied. The spatial resolution was 0.2 mm. By comparison with a 0.1 mm resolution in a 1-D preparation, we verified that the spatial resolution was high enough. Tissue conductivity values were  $\sigma_{eT} = 0.12$ ,  $\sigma_{eL} = 0.3$ ,  $\sigma_{iT} = 0.03$  and  $\sigma_{iL} = 0.3 \text{ Sm}^{-1}$ , with subscript ‘e’ for extracellular, ‘i’ for intracellular, ‘T’ for transverse, and ‘L’ for longitudinal [7]. In each experiment, the model was integrated until a quasi-stable distribution of  $V_m$  was obtained.

Even in the absence of perfusion, extracellular  $K^+$  in ischemic myocardium appears to move to the normal myocardium by a diffusive process, resulting in a concentration gradient and therefore a gradient in resting  $V_m$  [9]. This idea is illustrated in Fig. 2. We [6] have previously proposed to describe this process using a diffusion equation with additional source and sink terms:

$$\frac{\partial [K^+]_o}{\partial t} = D \nabla^2 [K^+]_o + S + P \quad (1)$$

where  $D$  ( $\text{m}^2/\text{s}$ ) is a diffusion constant. The source term  $S$  represents the net efflux of  $K^+$  from the cells. The sink term  $P$  represents the removal of  $K^+$  by perfusion:  $P = 0$  for ischemic myocardium, and  $P = g \cdot (5.4 \text{ mM} - [K^+]_o)$  elsewhere (including the blood), with  $g$  a constant. The source term  $S$  is due to net  $K^+$  efflux in ischemic tissue. It depends on  $V_m$ , and thus indirectly on  $[K^+]_o$ . In this study, we neglect this (minor) dependence. Instead, we assume a constant uniform  $S$  throughout the metabolically affected area.

The diffusion process described by (1) can approach an asymptotic steady state, in which  $\partial [K^+]_o / \partial t = 0$ , so

$$\nabla^2 [K^+]_o = -\frac{S}{D} \quad (2)$$

in the ischemic zone. Using the approximation  $g = \infty$ , we can impose a Dirichlet boundary condition  $[K^+]_o = 5.4 \text{ mM}$  on the border of the hypoxic zone (“metabolic border”). For

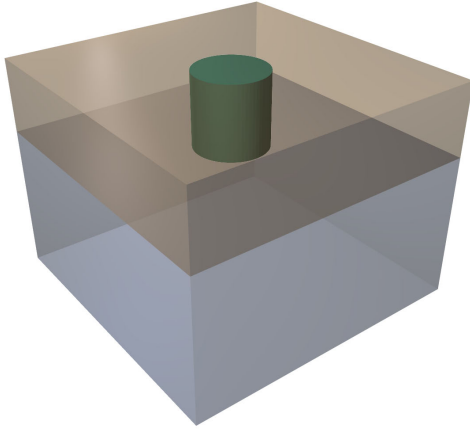


Fig. 1. Three-dimensional simulation setup. The tissue block (top) is 4 cm wide, 4 cm long, and 1 cm thick. It floats on top of a tissue bath of 2 cm thickness. In the tissue, a cylindrically shaped ischemic zone of varying diameter was present; in this example the diameter was 1 cm.

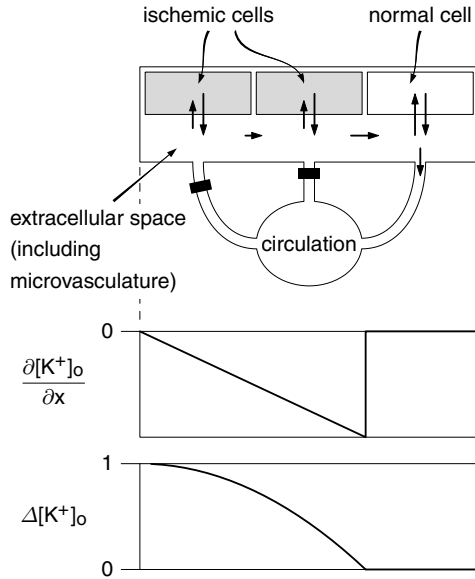


Fig. 2. Schematic representation of  $K^+$  loss and diffusion. The left side of each plot represents the center of the ischemic zone, which may be assumed to be symmetric. The upper diagram shows two ischemic cells and one normal cell. They are surrounded by an extracellular space, which includes the interstitium, vasculature, and lymphatic system. The ischemic cells extrude more  $K^+$  than they can absorb. Moreover, the surplus  $K^+$  ions cannot immediately enter the circulating blood. Instead, they must travel through the interstitial space and perhaps arrested but not drained (micro)vessels to the normally perfused tissue, where they are taken up by the circulation. The lower panels show the  $[K^+]_o$  distribution and its spatial gradient that follow from this hypothesis.

a one-dimensional model or a circular ischemic zone in two dimensions the solution to this equation is a parabolic profile. The peak value of this profile is

$$[K^+]_{o,c} = 5.4 \text{ mM} + \frac{1}{2} \frac{S}{D} R^2 \quad (3)$$

where  $R$  is the radius of the ischemic zone. By fitting this equation to experimental data [9], we obtained the estimate  $S/D = 2.5 \text{ mM/cm}^2$ .

### III. RESULTS

Fig. 3, panels a and b, show the configurations of  $\phi_e$  and  $I_m$  seen from inside the preparation. The pattern of  $\phi_e$ , with maxima along the fiber orientation, is similar to that in propagating activation [7]. The maximum of positive (outward)  $I_m$  is also found in the direction of the fibers, with a maximum on the metabolic border. Profiles of  $[K^+]_o$ , resting  $V_m$ ,  $\phi_e$ , and  $I_m$  are shown in panels e–h, both along and across the local fiber orientation, in a plane halfway the thickness of the tissue slab. The parabolic profile of  $[K^+]_o$  was predefined, according to our diffusion model in equilibrium state, using an (unrealistic)  $[K^+]_{o,c} = 12 \text{ mM}$ . The profile of  $I_m$  shows that the negative (i.e. inward) current is somewhat larger near the borders of the ischemic zone than in the center. A positive (outward) current was found at the border. The peak of this positive current coincided with the metabolic border. Outward currents were found both outside and inside the metabolically affected area.

The left and middle columns of Fig. 4 compare ischemic zones of two different sizes.  $[K^+]_{o,c}$  was determined according to (3), so it was higher in the larger zone. Consequently,  $\phi_e$  and  $I_m$  were larger. The larger zone also had a more important effect on the reference potential. The resulting shift in  $\phi_e$  caused the zero crossing (along the fiber orientation), which defines the “electrophysiological border” of the ischemic area, to shift approximately 2 mm inward with respect to the metabolic border.

Repeating this analysis for larger zones, and assuming that  $[K^+]_{o,c}$  can not become larger than 14 mM (in phase I of ischemia), we found that the maximum attainable  $I_m$  was  $0.25 \mu\text{A/mm}^3$ . This occurred at a radius of 26 mm. For larger zones, we assume that there is a plateau of  $[K^+]_o$  in the center, and that  $[K^+]_o$  varies in a 26 mm wide boundary.

The right column of panels in Fig. 4 shows a similar analysis for a flat profile of  $[K^+]_o$ . The concentration is arbitrary in this case. Due to electrotonic interaction, the resulting profile of  $V_m$  is not flat, but has a rounded foot, and  $I_m$  remains finite. However, the peak  $I_m$  is an order of magnitude larger than that resulting from a parabolic profile of  $[K^+]_o$ , and  $I_m$  is zero in a large part of the ischemic zone.

In order to relate the current magnitude that was found to that required for induction of arrhythmia, we also computed propagating action potentials. Fig. 5 shows the ionic current density and total membrane current density for a position in the normal tissue, and for a position in the ischemic zone. The latter position had a  $[K^+]_o$  that inhibited the fast Na current, but still allowed propagation supported by the slower Ca current. The resulting maximum current density is more than an order of magnitude smaller than in normal tissue. In particular, the current density associated with the approaching wavefront is only  $3 \mu\text{A/mm}^3$ .

### IV. DISCUSSION

Myocardial ischemia causes an “injury current” to flow between the ischemic and non-ischemic tissue. The question whether this current is large enough to induce ectopic activation has not yet been resolved. In this study, we

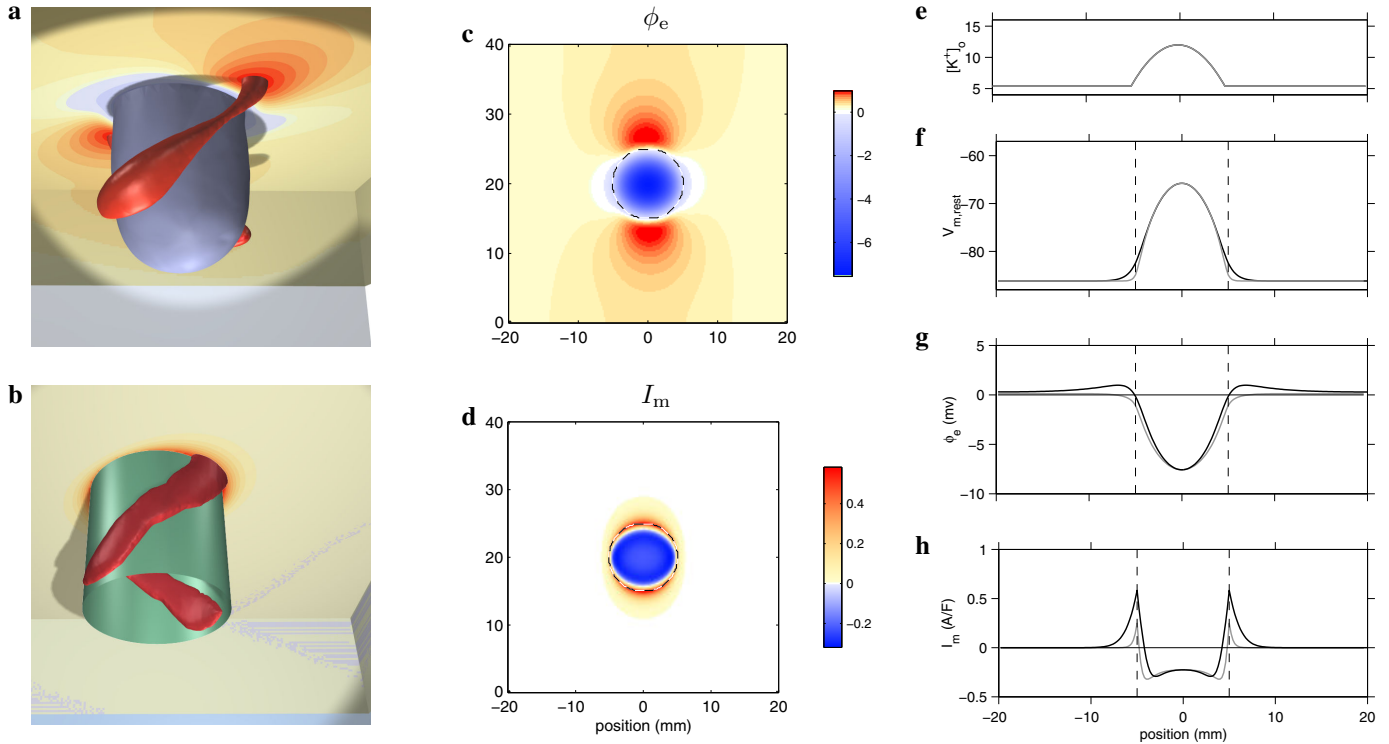


Fig. 3. **Panel a:** Distribution of  $\phi_e$  on the surface of the tissue preparation, seen from within. The color scale ranges from blue through yellow to red; blue is negative, yellow and red are positive. Isopotential surfaces are shown for +1 and -1 mV. The positive isopotential surface illustrates the effect of transmural fiber rotation. **Panel b:** Distribution of  $I_m$  in the same experiment. The green cylinder indicates the metabolic border, the red filaments are iso-current surfaces for near-maximum  $I_m$ . They cross the metabolic border. **Panels c and d** show  $\phi_e$  and  $I_m$  in a plane in the middle of the wall. The fiber orientation is vertical in this representation. The ischemic region, a “pillbox” with a diameter of 10 mm, is located in the middle. The metabolic border is indicated with a dashed line. **Panels e-h** show profiles of  $[K^+]_o$ , resting  $V_m$ , resting  $\phi_e$ , and resting  $I_m$  along (black) and across the fibers (gray) from the same plane as panels c and d. The vertical dashed lines indicate the metabolic border.

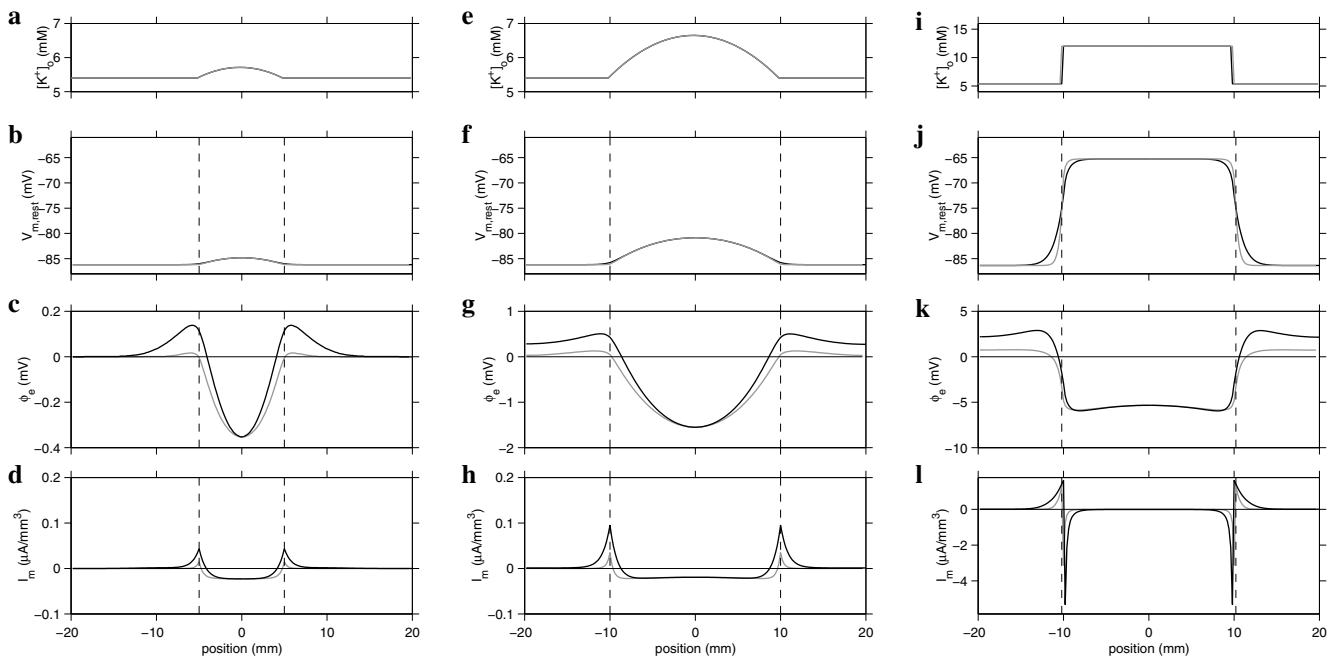


Fig. 4. **Panels a-d:** profiles of  $[K^+]_o$ , resting  $V_m$ , resting  $\phi_e$ , and resting  $I_m$  for an ischemic zone with radius 5 mm. For legends see Fig. 3, panels e-h. **Panels e-h:** the same profiles, for an ischemic zone with radius 10 mm. **Panels i-l:** the same profiles, for a flat profile of  $[K^+]_o$ .

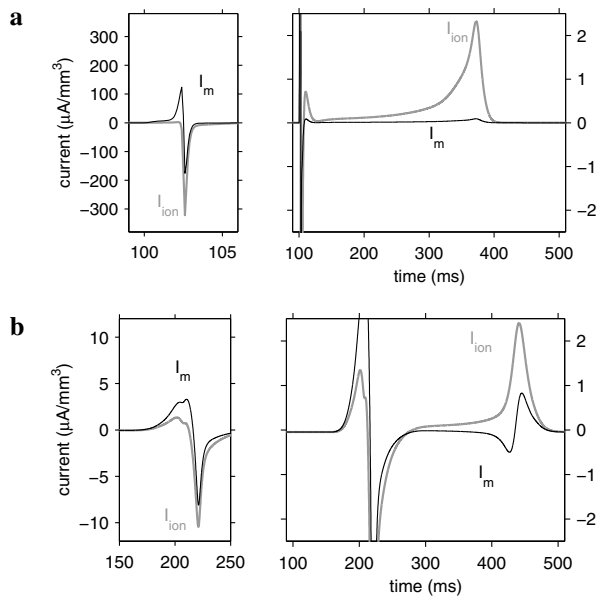


Fig. 5. Membrane current density and ionic current density for propagating action potentials in normal (panel a) and ischemic (panel b) tissue. (the diastolic injury current here in the center of the ischemic zone is about  $-0.05 \mu\text{A}/\text{mm}^3$ , which is much smaller than the propagation-related currents)

have quantitatively estimated the value and location of the depolarizing injury current that occurs during diastole in the border of the ischemic zone.

According to our simulations, the diastolic injury current would have a maximum value of  $0.25 \mu\text{A}/\text{mm}^3$ , which would occur precisely on the metabolic border. Part of the outward injury current would occur inside the metabolically affected area, where the activation threshold is lower than in normal tissue.

The amplitude of the diastolic injury current is determined by the slope of the  $[\text{K}^+]_o$  profile, and thus depends on the diffusion constant for  $\text{K}^+$  in the extracellular domain. Since the diffusion of  $\text{K}^+$  is thought to be facilitated by pulsative flow [9], microcirculatory contraction would limit diffusion, increase the steepness of the  $[\text{K}^+]_o$  profile, and thus increase the diastolic injury current.

A larger injury current than the  $0.25 \mu\text{A}/\text{mm}^3$  estimated here may also be present in the subendocardium. Due to diffusion of oxygen from the cavity, there is a thin subendocardial layer where ischemia is less severe. This layer may actually survive while infarction occurs in other layers. The transmural gradient of  $[\text{K}^+]_o$  was found to be much steeper in this layer than the lateral gradient [10]. This could allow an injury current up to  $2 \mu\text{A}/\text{mm}^3$  if the cells are well coupled. Uncoupling during ischemia would reduce this current.

Ectopic foci occur most often after a “large negative T wave” caused by delayed repolarization in the ischemic zone [11]. If the ischemic tissue is still depolarized and the normal tissue already repolarized, a membrane potential difference in the order of 70 mV may exist over a very short spatial interval. This too results in a current of  $2 \mu\text{A}/\text{mm}^3$  [11].

The arrhythmogenicity of a depolarizing transmembrane current can be judged by comparing its magnitude to the current associated with a propagating wavefront. Coronel et al. [12] have shown that the current density associated with propagation in healthy myocardium is in the order of  $100 \mu\text{A}/\text{mm}^3$ . In our simulation, the transmembrane current associated with normal propagation was also approximately  $100 \mu\text{A}/\text{mm}^3$ , but an approaching Ca-carried wavefront generated a current density of only  $3 \mu\text{A}/\text{mm}^3$ .

The maximum injury current of  $0.25 \mu\text{A}/\text{mm}^3$  that follows from our model does not seem sufficient to cause premature ectopic activation in myocytes. However, the steepness of the parabolic  $[\text{K}^+]_o$  profile, its peak value, and the size of the plateau depend on the diffusion constant  $D$ . This constant may decrease substantially when microvascular vasoconstriction occurs. The flat  $[\text{K}^+]_o$  profile represents the limiting case where  $D = 0$ . In this limit, the diastolic injury current could be as large as  $2 \mu\text{A}/\text{mm}^3$  (Fig. 4). The current may also be larger in the subendocardium, coinciding with Purkinje cells, which have a lower threshold for activation.

## REFERENCES

- [1] E. Carmeliet, “Cardiac ionic currents and acute ischemia: From channels to arrhythmias,” *Physiol. Rev.*, vol. 79, no. 3, pp. 917–1017, 1999.
- [2] J. L. Hill and L. S. Gettes, “Effect of acute coronary artery occlusion on local myocardial extracellular  $\text{K}^+$  activity in swine,” *Circulation*, vol. 61, no. 4, pp. 768–778, 1980.
- [3] M. J. Janse and A. G. Kléber, “Electrophysiological changes and ventricular arrhythmias in the early phase of regional myocardial ischemia,” *Circ. Res.*, vol. 49, pp. 1069–1081, 1981.
- [4] P. R. Johnston, D. Kilpatrick, and C. Y. Li, “The importance of anisotropy in modeling ST segment shift in subendocardial ischaemia,” *IEEE Trans. Biomed. Eng.*, vol. 48, no. 12, pp. 1366–1376, 2001.
- [5] B. Hopenfeld, J. G. Stinstra, and R. S. MacLeod, “Mechanism for ST depression associated with contiguous subendocardial ischemia,” *J. Cardiovasc. Electrophysiol.*, vol. 15, no. 10, pp. 1200–1206, 2004.
- [6] M. Potse, R. Coronel, S. Falcao, A.-R. LeBlanc, and A. Vinet, “The effect of lesion size and tissue remodeling on ST deviation in partial-thickness ischemia,” *Heart Rhythm*, vol. 4, no. 2, pp. 200–206, 2007.
- [7] M. Potse, B. Dubé, J. Richer, A. Vinet, and R. M. Gulrajani, “A comparison of monodomain and bidomain reaction-diffusion models for action potential propagation in the human heart,” *IEEE Trans. Biomed. Eng.*, vol. 53, no. 12, pp. 2425–2435, 2006.
- [8] K. H. W. J. ten Tusscher, D. Noble, P. J. Noble, and A. V. Panfilov, “A model for human ventricular tissue,” *Am. J. Physiol. Heart Circ. Physiol.*, vol. 286, pp. H1573–H1589, 2004.
- [9] R. Coronel, J. W. T. Fiolet, F. J. G. Wilms-Schopman, A. F. M. Schaapherder, T. A. Johnson, L. S. Gettes, and M. J. Janse, “Distribution of extracellular potassium and its relation to electrophysiologic changes during acute myocardial ischemia in the isolated perfused porcine heart,” *Circulation*, vol. 77, no. 5, pp. 1125–1138, 1988.
- [10] R. L. Wilensky, J. Tranum-Jensen, R. Coronel, A. A. Wilde, J. W. T. Fiolet, and M. J. Janse, “The subendocardial border zone during acute ischemia of the rabbit heart: an electrophysiologic, metabolic, and morphologic correlative study,” *Circulation*, vol. 74, pp. 1137–1146, 1986.
- [11] M. J. Janse, F. J. L. van Capelle, H. Morsink, A. Kléber, F. Wilms-Schopman, R. Cardinal, C. Naumann d’Almoncourt, and D. Durrer, “Flow of “injury” current and patterns of excitation during early ventricular arrhythmias in acute regional myocardial ischemia in isolated porcine and canine hearts; evidence for two different arrhythmogenic mechanisms,” *Circ. Res.*, vol. 47, no. 2, pp. 151–165, Aug. 1980.
- [12] R. Coronel, F. J. G. Wilms-Schopman, J. R. de Groot, M. J. Janse, F. J. L. van Capelle, and J. M. T. de Bakker, “Laplacian electrograms and the interpretation of complex ventricular activation patterns during ventricular fibrillation,” *J. Cardiovasc. Electrophysiol.*, vol. 11, pp. 1119–1128, 2000.